

Physical Studies in III-Nitride Semiconductor Alloys

Vedam Rama Murthy¹, Alla Srivani^{2,*} and G Veera raghavaiah³

¹T.J.P.S College, Guntur, Andhra Pradesh., India

²Vasireddy Venkatadri Institute of Technology (VVIT), Engineering College, Andhra Pradesh, Rayalaseema University, India

³PAS College, Pedanandipadu., India

Received: 21 Sep. 2016, Revised: 12 Nov. 2016, Accepted: 12 Dec. 2016.

Published online: 1 Jan. 2017.

Abstract: Many theoretical and experimental works are made on the wurtzite phase of indium nitride (InN), gallium nitride (GaN), aluminum nitride (AlN), and their Ternary alloys. On the other side, few experimental data exist for their cubic phases where as theoretical studies show they are performing more interesting. Inclusive depiction of III-Nitride Semiconductors is demonstrated and consequence of existent Research is emphasised. The Electrical and Optical properties of III-Nitrides from binary Semiconductors are appraised using the Principle of additivity comprising quadratic expressions. The Electrical and Optical properties learned in this group restrain Refractive index, Optical polarizability, Absorption coefficient and Energy gap. A similarity of these data is made with reported information facts wherever attainable. The worth of current displayed method build from refractive indices with out need for refined experimental methods is stressed. The beneficial of this Nitride Group Alloys is also summarized.

Keywords: Semiconductor alloys, Nitride semiconductor alloys, III-V Nitide Alloys and Physical properties.

1 Introduction

III-nitrides have gained a significant position in the science and technology of compound semiconductors, as well as in modern electronic and optical devices. The III-Nitride semiconductors have attracted much attention over recent years because of their potential applications in technological devices. This is due mainly to the fact that the energy gap can be tuned over a wide spectral range from the visible to the ultraviolet region of the electromagnetic spectrum. Although the zincblende and wurtzite structures are present in the GaN, AlN, and InN semiconductors, it has been demonstrated experimentally that wurtzite is the most stable structural phase of these compounds. Moreover, due to their high chemical and thermal stability, the III-Nitrides are ideal candidates for applications under extreme conditions such as high temperature applications.

The hexagonal wurtzite structure is extensively utilized because all the III-nitride semiconductors and their alloys exhibit a direct band gap energy, which results in a high emitting performance. Due to the remarkable progress in epitaxial growth technology, high quality samples of these compounds can be produced. III-Nitrides have recently attracted attention as a promising material class for high-power, high frequency microelectronic applications at

elevated temperatures. They possess large band gaps, relatively small effective masses in the conduction band minimum, large offsets to the conduction band satellite valleys, and high polar optical phonon frequencies¹.

2 Nitrides

We present a study of the structural, Optical and electrical properties of the wurzite structure AlN, GaN, InN semiconductors and their related alloys, GaAs_xN_{1-x}, Al_xGa_{1-x}N, Al_xIn_{1-x}N, InAs_xN_{1-x}, GaP_xN_{1-x} and In_xGa_{1-x}N. The analysis was made by calculating the total energy. First, we analyzed the binary compounds, GaN, AlN, and InN, and then their related alloys, Al_xGa_{1-x}N and In_xGa_{1-x}N. The values of the lattice parameters for the Al_xGa_{1-x}N alloy decrease when the Al content is increased. This is due to the fact that the size of the Al atom is smaller than the Ga atom. This is not the case for the internal parameter, *u*, in which we observe an increase of this parameter when we increase the Al content in the alloy.

Recent improvements in the molecular beam epitaxy (MBE) technique have led to the availability of high quality InN films. Hagan et al and Baranov et al. were the first to

*Corresponding author E-mail: allasrivani@gmail.com

demonstrate experimentally the existence of the $\text{Al}_x\text{Ga}_{1-x}\text{N}$ alloy. III-V wide band gap nitrides include aluminum nitride (AlN), gallium nitride (GaN), indium nitride (InN) and their alloys. All of these are compounds of nitrogen which is the smallest element from group V in the periodic table. Very strong chemical bonds result within the III-nitride material system due to the large difference in electro-negativity between group III and V elements².

2.1 $\text{Al}_x\text{Ga}_{1-x}\text{N}$

$\text{Al}_x\text{Ga}_{1-x}\text{N}$ alloys are the materials most widely used in the fabrication of III-Nitride FETs. The III-nitride semiconductor is one of the most promising optoelectronic materials because it possesses excellent mechanical properties such as high melting point, high hardness, high thermal conductivity, and large bulk modulus, etc. Furthermore, it has many outstanding optical properties such as lower dielectric permittivity and wide range energy band gap covering a spectral range from the visible to the near ultraviolet. Most nitride crystal materials have direct energy band gap resulting in high emitting performance. The main applications of III-nitride semiconductor include high efficiency light emitting diodes (LEDs) for displays and laser diodes (LD) for high-density optical storage and high-resolution laser printing. In addition, bright blue LEDs based on III-nitride semiconductors have already paved the way for full-color displays and for mixing three primary colors to obtain white light for illumination.

Two basic crystal structures of III-nitride alloys are used today: hexagonal wurtzite structure and cubic zinc blende structure. Wurtzite structure is widely applied due to its direct energy band gap in III-nitride semiconductors. The AlGaN is extensively used in barrier layer, cladding layer, or distributed Bragg reflector (DBR) in semiconductor laser having quantum well or as active layer in short wavelength (ultraviolet) LEDs and semiconductor lasers. The melting temperature of $\text{Al}_x\text{Ga}_{1-x}\text{N}$ greatly increased as the Al content x increased because the expected melting temperature of AlN is higher than 3000°C. Further technical development to achieve such high temperatures is required to synthesize more Al rich $\text{Al}_x\text{Ga}_{1-x}\text{N}$ single crystals from their melts. The first growth of $\text{Al}_x\text{Ga}_{1-x}\text{N}$ bulk crystals with Al concentration up to 30% was reported using a high-pressure, anvil-growth technique. Most recently, it was succeeded in obtaining high quality $\text{Al}_x\text{Ga}_{1-x}\text{N}$ single crystals with the Al content x between 0.5 and 1, by performing the synthesize from the solution in Ga melt in a nitrogen-gas system. The high-nitrogen-gas system consists of a compressor, high-pressure chamber of 40 mm internal diameter with the internal, three-zone furnace, and an electronic system for programming and stabilizing both pressure and temperature³.

2.2 $\text{In}_x\text{Ga}_{1-x}\text{N}$

A technologically important example is band gap engineering where the width of the band gap is controlled by the alloy composition x . A new and technologically very interesting semiconductor alloy system where this effect is utilized is $\text{In}_x\text{Ga}_{1-x}\text{N}$. This alloy is used, e.g., as an active region in GaN-based optoelectronic devices and ~assuming complete miscibility! Allows to tune the band gap between 1.9 eV ~InN and 3.5 eV ~GaN, i.e., between the infrared and ultraviolet region of the optical spectrum. An important issue for $\text{In}_x\text{Ga}_{1-x}\text{N}$ alloys is homogeneity: Experimentally it has been found that these alloys are often unstable against phase separation, spatial fluctuations in the In concentration, or partial ordering.

These effects have been shown to strongly affect the luminescence efficiency. It is therefore crucial to get a deeper insight into the energetic and local atomic structure of $\text{In}_x\text{Ga}_{1-x}\text{N}$ alloys. A unique feature of group III nitrides compared to traditional semiconductors is their large ionicity. $\text{In}_x\text{Ga}_{1-x}\text{N}$ alloys with energies from 0.7 to 3.4 eV can be tuned from ultraviolet to near infrared region by varying the In content. Figure 1.3 shows the band gap energy verses Ga content in $\text{In}_x\text{Ga}_{1-x}\text{N}$ alloys which covers almost the whole solar spectrum range. One can get the useful part of solar spectrum by varying Ga content between 0 and 0.63 in the $\text{In}_x\text{Ga}_{1-x}\text{N}$ alloys, which varies band gap energies from 0.7 to 2.4 eV.

$\text{In}_x\text{Ga}_{1-x}\text{N}$ with higher content of indium showed a broad PL emission and large tails of absorption. UV- VIS Spectroscopy and photoluminescence measurements have been used to study Optical properties of $\text{In}_x\text{Ga}_{1-x}\text{N}$ films grown by CVD. In the development field of new materials the compound semiconductors continue being an area of great interest and rapid expansion. Scanning electron microscopy and X-Ray diffraction were used to characterize structure of $\text{In}_x\text{Ga}_{1-x}\text{N}$ thin films. InGaN based, blue and green light emitting diodes (LEDs) have been successfully produced over the past decade. But the progress of these LEDs is often limited by the fundamental problems of InGaN such as differences in lattice constants, thermal expansion coefficients and physical properties between InN and GaN. This difficulty could be addressed by studying pure InN and $\text{In}_x\text{Ga}_{1-x}\text{N}$ alloys. Ga-rich $\text{In}_x\text{Ga}_{1-x}\text{N}$ (x . 0.4) epitaxial layers were grown by metal organic chemical vapor deposition (MOCVD). X-ray diffraction (XRD) measurements showed $\text{In}_x\text{Ga}_{1-x}\text{N}$ films with $x=0.37$ had single phase. Phase separation occurred for $x \sim 0.4$. To understand the issue of phase separation in Ga-rich $\text{In}_x\text{Ga}_{1-x}\text{N}$, studies on growth of pure InN and In-rich $\text{In}_x\text{Ga}_{1-x}\text{N}$ alloys were carried out. InGaN alloys have great potential for use in solar cells for space applications as they offer a higher degree of resistance to radiation damage.

InGaN based blue-green LEDs and LDs have already been successfully fabricated that employ $\text{In}_x\text{Ga}_{1-x}\text{N}$ films with lower In contents of about $x < 0.2$. Recently, the properties of $\text{In}_x\text{Ga}_{1-x}\text{N}$ films with a higher In content $x > 0.5$ have

also been investigated by several research groups. InGaN based, blue and green light emitting diodes (LEDs) have been produced successfully over the past decade. But due to the large differences in lattice constants and thermal expansion coefficients and mechanical properties between InN and GaN, the progress of these LEDs is limited. This difficulty could be addressed by studying pure InN and $\text{In}_x\text{Ga}_{1-x}\text{N}$ alloys. Also it is useful to get information about the band gap energy of these materials. In this context systematic studies had been made on the growth and characterization of InN and $\text{In}_x\text{Ga}_{1-x}\text{N}$ alloys.

Although there are many techniques to grow III-nitrides but metal organic chemical vapor deposition (MOCVD) and molecular beam epitaxy (MBE) are the major techniques among them. In MBE growth, the constituent elements of III-nitrides are deposited in the form of molecular materials on a heated substrate to form an epitaxial layer. The low growth temperature and lack of sufficient radical nitrogen atoms are the main problems for MBE growth of III-nitrides. As a result, it has been very difficult to obtain p-type materials by MBE, which limits its use for producing light emitting structures based on III-nitrides.

Nevertheless, MBE has been very successful in producing some unique polar structures such as field effect transistors (FETs), in which p-type material is avoided. Furthermore it had been a successful technique to grow InN, p-type InN and In-rich InGaN epitaxial layers that require low growth temperature. On the other hand MOCVD technology is an efficient technique to grow III-nitride materials and devices, which require high growth temperature. MOCVD utilizes metal organic sources from group III-elements.

The group V element is usually a hydride such as ammonia (NH_3) to provide reactive nitrogen. Typically the hydride reacts with the metal organic source in hydrogen or nitrogen ambient under proper temperature and pressure conditions. Molecules of required semiconductor material are produced, which then adsorbs on the substrate surface to produce an epitaxial layer. Most of the materials mentioned in this dissertation were grown by a home built metal organic chemical vapor deposition (MOCVD) system⁴.

2.3 $\text{Al}_x\text{In}_{1-x}\text{N}$

$\text{Al}_x\text{In}_{1-x}\text{N}$ alloys have a wide range of band gap energies that match almost the entire solar spectrum and can be used in the development of solar cells with 50% efficiency. This compound also is difficult to grow and characterize owing to the large mismatch of the InN and AlN lattices. For $\text{Al}_x\text{In}_{1-x}\text{N}$ that is 0.047 0.011 angstrom for the lattice constant and -0.117 0.026 angstrom for the c lattice constant. For $\text{Al}_x\text{In}_{1-x}\text{N}$ that is 0.063 0.014 angstrom for the lattice constant and -0.160 0.015 angstrom for the c lattice constant. Two basic crystal structures of III-nitride alloys are used today: hexagonal wurtzite structure and cubic zinc blende structure. Wurtzite structure is widely applied due to

its direct energy band gap in III-nitride semiconductors. The III-nitride ternary alloys often used at present include AlGaIn, InGaIn, and AlInN. Depending on the composition ratio of the III-group elements, the energy band gap of III-nitride ternary alloys is tunable from 0.77 eV (InN) to 3.42 eV (GaN) and to 6.25 eV (AlN)⁵.

2.4 $\text{GaAs}_x\text{N}_{1-x}$

Electron cyclotron resonance-metal organic molecular beam epitaxy has been used to deposit GaN and $\text{GaAs}_x\text{N}_{1-x}$ [$0 < x < 1$] layers on various substrates. Alloying is a commonly accepted method to tailor properties of semiconductor materials for specific applications. Only a limited number of semiconductor alloys can be easily synthesized in the full composition range. Such alloys are, in general, formed of component elements that are well matched in terms of ionicity, atom size, and electro negativity. In contrast there is a broad class of potential semiconductor alloys formed of component materials with distinctly different properties. In most instances these mismatched alloys are immiscible under standard growth conditions.

The alloys are amorphous in the composition range of 0.17, and to the upward movement of the valence band for alloys with $x < 0.2$. The unique features of the band structure offer an opportunity of using $\text{GaAs}_x\text{N}_{1-x}$ alloys for various types of solar power conversion devices. The dilute $\text{GaAs}_x\text{N}_{1-x}$ alloys (with x up to 0.05) have exhibited many unusual properties as compared to the conventional binary and ternary semiconductor alloys. We report on a new effect in the $\text{GaAs}_x\text{N}_{1-x}$ alloy system in which electrically active substitution group IV donors and isoelectronic N atoms passivity each other's activity.

This mutual passivity occurs in dilute $\text{GaAs}_x\text{N}_{1-x}$ doped with group IV donors through the formation of nearest neighbor IV Ga-NAs pairs when the samples are annealed under conditions such that the diffusion length of the donors is greater than or equal to the average distance between donor and N atoms. The passivity of the shallow donors and the NAs atoms is manifested in a drastic reduction in the free electron concentration and, simultaneously, an increase in the fundamental band gap. This mutual passivity effect is demonstrated in both Si and Ge doped $\text{GaAs}_x\text{N}_{1-x}$ alloys⁶.

2.5 $\text{InAs}_x\text{N}_{1-x}$

A series of growths conducted at different substrate temperatures and III-V ratios is analyzed by x-ray Diffraction (XRD) to determine composition. A metastable $\text{InAs}_x\text{N}_{1-x}$ alloy plus pure InAs are obtained for temperatures in the range 450–500 °C and total ratio of approximately unity. The InAs fraction in the alloy phase increases at lower temperatures, the maximum observed is 13%. For higher temperatures or higher III-V ratio only

separated phases of InAs and InN are found. The objective of this joint research is to explore new III-V compound

The objective of this joint research is to explore new III-V compound semiconductors incorporating nitrogen and other group V elements, such as $\text{GaP}_x\text{N}_{1-x}$ and $\text{InAs}_x\text{N}_{1-x}$. These materials are expected to exhibit very novel electronic properties such as very narrow or even negative band gap energy, and hence are electronically metals even though their constituents and atomic structures are those of semiconductors. These peculiar features can be applied in fabricating light detectors and light sources in the far IR region and in designing totally new classes of optical and electronic devices. Possible experimental realizations of $\text{AlAs}_x\text{N}_{1-x}$ and $\text{GaAs}_x\text{N}_{1-x}$ alloys are explored.

Growths were conducted to test whether the pseudo binary alloys III-In $\text{As}_x\text{N}_{1-x}$ could be formed by providing As_2 and excess Group III fluxes in a plasma-source nitride epitaxial growth process based on Si(1 1 1) substrates. Incorporation of several atomic percent of As occurs at typical III-V Nitrogen growth temperatures. However, X-ray and Transmission Electron Microscopy (TEM) analysis show that disordered phases are present and that the incorporated As is not purely substitution on N sub lattice sites.

A pronounced surfactant effect of As in the growth of GaN is demonstrated, with the surface roughness decreasing one order of magnitude. Another approach, using “digital” alloys of GaAsN formed by alternating beam epitaxy on GaAs (1 0 0) has demonstrated incorporation of several atomic percent of N in GaAs. High-resolution X-ray rocking curves and TRANSMISSION ELECTRON MICROSCOPY (TEM) images of the digital alloy are provided⁷.

2.6 $\text{GaP}_x\text{N}_{1-x}$

The behavior of $\text{GaP}_x\text{N}_{1-x}$ is contrasted with that of $\text{Al}_x\text{Ga}_{1-x}\text{As}$ and $\text{In}_x\text{Ga}_{1-x}\text{As}$ with respect to irregular and regular alloy behavior. It is proposed that $\text{GaP}_x\text{N}_{1-x}$ behave as heavily nitrogen doped semiconductors rather than dilute nitride alloys and that their abnormal or irregular alloy behavior is associated with impurity band formation that manifests itself in the giant bowing and poor transport properties characteristic of these materials. $\text{GaP}_x\text{N}_{1-x}$ samples were observed to be more efficient during the hydrogen production process than the pure GaP samples.

Core level spectroscopy was used to study the surfaces of the corroded $\text{GaP}_x\text{N}_{1-x}$ samples. At all energies, the uncorroded nitrogen spectra for the $\text{GaP}_x\text{N}_{1-x}$ ($x = 0.02$) sample shows two peaks, one corresponding to N bonded to Ga in the bulk, the other to NO_x and NH_x on the surface. The energy and composition of the direct to indirect band gap cross over in $\text{GaP}_x\text{N}_{1-x}$ significantly influences its potential for optoelectronic devices, such as solar cells and light emitting diodes, however considerable discrepancies still remain in the literature with regard to the precise value

of the crossover composition x_c . We revisit this issue in $\text{GaP}_x\text{N}_{1-x}$ films epitaxially grown on substrates⁸.

Method 1

$$A_{12} = A_1 * x + A_2 * (1-x) + 1/1000 * \text{SQRT} (A_1 * A_2 * x * (1-x)) \quad (1)$$

Method 2

$$A_{12} = A_1 * x + A_2 * (1-x) + 1/1000 * \text{SQRT} (A_1 * A_2 * x * (1-x)) \quad (2)$$

Method 3

$$A_{12} = A_1 * x + A_2 * (1-x) - 1/1000 * \text{SQRT} (A_1 * A_2 * x * (1-x)) \quad (3)$$

Method 4

$$A_{12} = A_1 * x + A_2 * (1-x) - 1/1000 * \text{SQRT} (A_1 * A_2 * x * (1-x)) \quad (4)$$

Additivity

$$A_{12} = A_1 * x + A_2 * (1-x) \quad (5)$$

Where A_{12} denotes Refractive index (n_{12}), Optical Polarizability (α_{m12}), Absorption coefficient (α_{12}) and Energy gap (E_{g12}) of Ternary Alloy. A_1 and A_2 denotes Refractive index (n), Optical Polarizability (α_m), Absorption coefficient (α) and Energy gap (E_g) of two binary compounds forming ternary compound.

3 Results and Discussion

The values of Refractive index, molecular polarizability, Absorption coefficient, Energy gap and Mobility of binary Semiconductors which are necessary for calculation are taken from CRC Hand book⁹.

3.1 Refractive Index

The refractive index of semiconductors represents a fundamental physical parameter that characterizes their optical and electronic properties. It is a measure of the transparency of the semiconductor to incident spectral radiation. In addition, knowledge of the refractive index is essential for devices such as photonic crystals, wave guides, solar cells and detectors¹⁰.

The refractive index values of Nitride Semiconductor alloys are evaluated by using additivity Principle and quadratic expressions of the equations 3.1 to 3.5 by replacing A by n the refractive index from the reported values of Refractive index of Binary Semiconductors¹¹.

Table 1 Refractive Index for Nitride Compounds

Compound	Refractive index n
AlN	2.15
GaN	2.30
InN	2.59

Table 1 represents Refractive index values of Binary Compounds AlN, GaN and InN

3.2 Optical polarizability

Optical Polarizability (α_m) is used to study Optical behavior of binary and Ternary Semiconductors belonging to III-Nitride Ternary Semiconductor alloys.

3.3 Optical polarizability of Binary Compounds

3.3.1 Lorentz-Lorenz relation

The mean Optical polarizability α_M for binary semiconductors is obtained by using Lorentz-Lorenz relation¹² given below

$$\alpha_m = \left(\frac{n^2 - 1}{n^2 + 1} \right) \frac{M}{\rho} \frac{3}{4\pi N} \quad (6)$$

Where M, N, n, ρ refer to Molecular weight, Avogadro number, Refractive index and density

New dispersion principle

The equation of motion of the electron may be written as

$$mZ + mbZ + \omega_0^2 mZ = eE_0 e^{i\omega t}$$

Here $E e^{i\omega t}$ refers to the electric force, $\omega = 2\pi\nu$, m is the electron mass,

ω_0 is Natural frequency of the electron and mbZ represents the damping term.

By solving the above equation, value of z will be obtained in the form as

$$Z = \frac{\left(\frac{e}{m}\right) E_0 e^{i\omega t}}{\omega_0^2 - \omega^2 + i\omega b}$$

Thus the moment induced (P) per unit volume will be

$$P = \Sigma Z e$$

$$P = \frac{v \left(\frac{e^2}{m}\right) E_0 e^{i\omega t}}{\omega_0^2 - \omega^2 + i\omega b}$$

Here v is Loschmidt number

Displacement vector is obtained as

$$D = E + 4\pi P$$

$$D = E + 4\pi \left[\frac{v \left(\frac{e^2}{m}\right) E_0 e^{i\omega t}}{\omega_0^2 - \omega^2 + i\omega b} \right]$$

$$D = E \left[1 + \frac{4\pi v \left(\frac{e^2}{m}\right)}{\omega_0^2 - \omega^2 + i\omega b} \right]$$

$$\frac{D}{E} = (n - ik)^2$$

$$\frac{D}{E} = \left[1 + \frac{4\pi v \left(\frac{e^2}{m}\right)}{\omega_0^2 - \omega^2 + i\omega b} \right]$$

The expression of n can be obtained by separating real and imaginary parts in above equations

$$\text{i.e } n = 1 + 2\pi \frac{e^2 v}{m} \frac{\omega_0^2 - \omega^2}{(\omega_0^2 - \omega^2)^2 + \omega^2 b^2}$$

If incident frequency $\omega < \omega_0$ then $\omega^2 b^2$ can be neglected. Thus above equation can be written as

$$\text{i.e } n = 1 + \frac{2\pi e^2 v}{m(\omega_0^2 - \omega^2)}$$

Rearranging the terms in above equation, we get

$$\left[\frac{1}{\lambda_0^2} - \frac{1}{\lambda^2} \right] = \frac{e^2 v}{2\pi c^2 m(n - 1)}$$

$$\frac{1}{\lambda^2} = \alpha + \frac{\beta}{(n - 1)}$$

Optical Polarizability of binary compounds can be calculated by using new dispersion relation¹³ by knowing α and β values

$$\frac{1}{\lambda^2} = \alpha + \frac{\beta}{n - 1} \quad (7)$$

Where $\alpha = \frac{1}{\lambda_0^2}$ and $\beta = \frac{e^2 v}{-2\pi m c^2}$

Dividing through out by β and rearranging the terms n_α

$$\frac{1}{n - 1} = \frac{1}{\beta \lambda^2} - \frac{\alpha}{\beta} \quad (8)$$

This equation is of the form Y=mx+c

$$\text{Lt}(\lambda \rightarrow \infty, \beta \lambda^2 \rightarrow 0)$$

$$\text{Hence } \frac{1}{n^{\infty}-1} = -\frac{\alpha}{\beta} = \gamma$$

$$\frac{1}{n_{\infty}-1} = \gamma$$

$$\frac{1+\gamma}{n_{\infty}} = \gamma$$

$$\frac{(1+\gamma)^2-1}{\gamma^2} = \frac{n_{\infty}^2-1}{n_{\infty}^2+2}$$

$$\frac{n_{\infty}^2-1}{n_{\infty}^2+2} = \frac{\gamma^2}{(1+\gamma)^2+2} \quad (9)$$

Substitute the value of $\frac{n_{\infty}^2-1}{n_{\infty}^2+2}$ in Lorentz-Lorenz formula, we get

$$\alpha_m = \left(\frac{(\gamma+1)^2 - \gamma^2}{(\gamma+1)^2 + 2\gamma^2} \right) \frac{M}{\rho} \frac{3}{4\pi N} \quad (10)$$

Where M, N and ρ are molecular weight, Avogadro number

and density of Binary Semiconductors and $v = \frac{\alpha}{\beta}$

Here α is Y-Intercept and β is the slope.

3.4 Absorption coefficient

Lorentz-Lorenz relation for solids is represented as follows

$$\left(\frac{n^2-1}{n^2+1} \right) = \frac{4\pi v \alpha_m}{3}$$

$$(n^2-1) = \frac{4\pi v \alpha_m \cdot 3}{3-4\pi v \alpha_m} = \left(\frac{1}{3} - \frac{1}{4\pi v \alpha_m} \right)^{-1}$$

$$\frac{1}{3} - \frac{1}{4\pi v \alpha_m} = \left(\frac{1}{n^2-1} \right)$$

$$\frac{12\pi v \alpha_m}{(n^2-1) = 3-4\pi v \alpha_m}$$

The absorption coefficient $\alpha = 2k = \frac{32\pi^3}{3v\lambda^4} (n-1)^2$

From the above two equations we get

$$\frac{(n^2-1)}{(n-1)^2} = \left(\frac{12\pi v \alpha_m}{3-4\pi v \alpha_m} \right)^1 \frac{32\pi^3}{3v\lambda^4 \alpha}$$

$$\frac{(n^2-1)}{(n-1)^2} = f(\text{consider})$$

$$\frac{n+1}{n-1} = f \quad \text{Or } n=f-1$$

$$\text{i.e } n = \left(\frac{\frac{128\pi^4 \alpha_m}{\alpha \lambda^4 (3-4\pi v \alpha_m)} + 1}{\frac{128\pi^4 \alpha_m}{\alpha \lambda^4 (3-4\pi v \alpha_m)} - 1} \right)$$

$$\text{i.e } \frac{n+1}{n-1} = \frac{128\pi^4 \alpha_m}{\alpha \lambda^4 (3-4\pi v \alpha_m)}$$

or

$$\alpha = \frac{128\pi^4 \alpha_m}{\alpha \lambda^4 (3-4\pi v \alpha_m)} \left(\frac{n-1}{n+1} \right)$$

$$\alpha = \frac{128\pi^4 \alpha_m}{\alpha \lambda^4 (3-4\pi v \alpha_m)} \left(\frac{n-1}{n+1} \right)$$

$$\alpha = \frac{128\pi^4 \alpha_m}{\lambda^4} \left(\frac{n-1}{n+1} \right) \left(\frac{M}{3M-4\pi N \rho \alpha_m} \right)$$

$\frac{N\rho}{M}$

Here $v = \frac{N\rho}{M}$

Where N is Avogadro number ρ is the density and M is molecular weight of the Semiconductor.

Thus the expression for absorption coefficient of binary semiconductor is given as

$$\alpha = \left(\frac{128\pi^4 \alpha_m}{\lambda^4} \right) \left(\frac{n-1}{n+1} \right) \left(\frac{M}{3M-4\pi N \rho \alpha_m} \right) \quad (11)$$

Where α_m , n, M, ρ and λ refer to the Optical Polarizability, Refractive index, molecular weight, density and wavelength of Binary semiconductors. N is Avogadro number.

Similarly for Ternary Semiconductors, the expression for absorption coefficient can be given as

$$\alpha = \left(\frac{128\pi^4 \alpha_{m12}}{\lambda^4} \right) \left(\frac{n_{12}-1}{n_{12}+1} \right) \left(\frac{M_{12}}{3M_{12}-4\pi N \rho_{12} \alpha_{m12}} \right) \quad (12)$$

Where α_{m12} , n_{12} , M_{12} and ρ_{12} are Optical Polarizability, refractive index, molecular weight and density of Ternary Semiconductor alloys and N is Avogadro number. They are calculated by using different additivity relations and Quadratic expressions.

3.5 Energy gap

The Electrical conductivity of Semiconductors depends on width of Energy Gap and it is affected by Dopant composition, Temperature, Pressure, Magnetic and Electrical fields. Indirect band gap Semiconductors is inefficient for emitting light. Semiconductors that have direct band gap are good light emitters. A wide band gap (WBG) semiconductor is a semiconductor with an energy band gap wider than about 2 eV, suitable for microwave devices. A narrow band semiconductor has energy band gap narrower than about 2 eV suitable for tunnel devices and infrared technology. Band gap is measured by both spectroscopic and conductivity methods.

3.5.1 Energy gap of Ternary semiconductors

The formula used for calculation of Energy gap of ternary semiconductors are given below

$$E_g = \left\{ \frac{28.8}{((2x_M - x_N)^2)^{\frac{1}{4}}} \left[\frac{1 - \Phi_{12}}{1 + 2\Phi_{12}} \right] \right\} \left[\frac{x_M}{x_N} \right]^2 \tag{13}$$

Where x_M and x_N are the electro negativities of the constituent atoms of ternary semiconductor

$$\Phi_{12} = \left[\frac{4\pi N}{3} \right] \left[\frac{\alpha_{M_{12}} \rho_{12}}{M_{12}} \right] \tag{14}$$

Where $\alpha_{M_{12}}$, ρ_{12} , M_{12} and N are optical polarizability, density, molecular weight and Avogadro number of ternary semiconductor Alloys.

The refractive index values of Binary Nitride compound semiconductors are taken from reference and are given in table 1. The refractive index values of Ternary semiconductor alloys are calculated by using different expressions of 1 to 3 for whole composition range ($0 < x < 1$) and are presented in tables from 2 to 5. These values are compared with literature reported data. It is found that calculated values are in good agreement with reported values. Graphs are drawn for all these alloys by taking their composition values on x axis and Refractive index values on y axis. These graphs are given from fig 1 to 2.

The refractive indices at various wavelengths for the binary semiconductors are taken from hand book of Optical constants of solids are presented in table 25 to 33 along with $\frac{1}{n-1}$ and $\frac{1}{\lambda^2}$ values. The graphs drawn between $\frac{1}{n-1}$ and $\frac{1}{\lambda^2}$ for these Semiconductors are shown in figures.

From these graphs intercept α values and the slope β of the straight line are determined and γ values are calculated. All these values are given from the table 6. The evaluated Optical Polarizabilities of Binary Semiconductors by using equation 8 are also from the table 6. The computed Optical polarizabilities by new dispersion relations are compared with reported values.

The values of Molecular weight (M), density (ρ) and refractive index (n) of the semiconductors which are required for evaluation of α_m are taken from CRC Hand book. The Energy Gap values of III-V Nitride Ternary Semiconductor Alloys of $Al_xGa_{1-x}N$ Ternary Semiconductor Alloy, $In_xGa_{1-x}N$ Ternary Semiconductor Alloy, $Al_xIn_{1-x}N$ Ternary Semiconductor Alloy, $GaAs_xN_{1-x}$ Ternary Semiconductor Alloy, $InAs_xN_{1-x}$ Ternary Semiconductor Alloy and GaP_xN_{1-x} Ternary Semiconductor Alloy are calculated by using 1, 2 and 3 of different Additivity Expressions and presented in tables from 4 to 8. These values are compared with Reported data. Graphs are drawn for the above III-V Nitride Ternary Semiconductor Alloys of $Al_xGa_{1-x}N$ Ternary Semiconductor Alloy, $In_xGa_{1-x}N$ Ternary Semiconductor Alloy, $Al_xIn_{1-x}N$ Ternary Semiconductor Alloy, $GaAs_xN_{1-x}$ Ternary Semiconductor Alloy, $InAs_xN_{1-x}$ Ternary Semiconductor Alloy and GaP_xN_{1-x} Ternary Semiconductor Alloy with variation of Dopant compositions and are given in fig.4 to .8. Calculated values of Energy gap is taken on x axis and their composition values are taken on y axis.

The refractive indices at various wavelengths for the binary semiconductors are taken from hand book of Optical constants of solids are presented in table 25 to 33 along with $\frac{1}{n-1}$ and $\frac{1}{\lambda^2}$ values. The graphs drawn between $\frac{1}{n-1}$ and $\frac{1}{\lambda^2}$ for these Semiconductors are shown in figures. From these graphs intercept α values and the slope β of the straight line are determined and γ values are calculated. All these values are given from the table 6. The evaluated Optical Polarizabilities of Binary Semiconductors by using equation 8 are also from the table 6. The computed Optical polarizabilities by new dispersion relations are compared with reported values.

Table 2 Energy gap of Nitride Compounds

Compound	Energy gap E_g^{12} e.v
AlN	6.02
GaN	3.20
InN	0.65

Table 2 represents Energy gap values of Binary Compounds AlN, GaN and InN

Table 3: Optical Polarizability of AlN

Compound	Energy Gap Eg (ev)	Wave Length Λ	Refractive Index N	$\frac{1}{n-1}$	$\frac{1}{\lambda^2}$	Optical Polarizability ¹⁰	
AlN	3.00	4133	2.146	0.872	5.8548	Calculated 264.3	Reported 250.7
	2.95	4200	2.212	0.825	5.669		
	2.81	4400	2.201	0.832	5.165		
	2.69	4600	2.191	0.839	4.726		
	2.58	4800	2.184	0.844	4.340		
	2.43	5100	2.174	0.851	3.845		

Table 3 represents Calculated Optical Polarizability value of AlN

Table 4 Energy GaP of BN

Wave length λ [(Å)] ¹⁰	$\frac{1}{\lambda^2}$ In (10) ⁸ (cms) ²	Refractive index value n	$\frac{1}{n-1}$	Optical polarizability α_m ([10]) ⁻²⁵ (cms) ³	Absorption coefficient (ω) ([10]) ⁻¹ cms ⁻¹	Energy Gap E_g^{12} e.v	
BN	3.07	4040	2.1109	90.02	6.127	Calculated 1.52	Reported 1.42
	2.86	4340	2.1107	90.03	5.309		
	2.66	4660	2.1105	90.05	4.605		
	2.47	5010	2.1103	90.07	3.984		
	2.30	5390	2.1101	90.08	3.442		
	2.14	5790	2.1098	90.11	2.983		
	1.99	6230	2.1095	90.13	2.576		

Table 4 represents Calculated Optical Polarizability value of BN

Table 5 Energy gap of Al_xGa_{1-x}N

Al Composition x	1-x	Energy gap Method-1 Ev	Energy gap Method-2 ev	Energy gap Method-3 ev	Energy gap Method-4 ev	Energy gap Additivity ev	Energy gap Reported E_g^{12} ev
0.00	1.00	1.77	1.77	1.77	1.77	1.77	1.77
0.25	0.75	2.33	2.34	2.33	2.33	2.33	2.32
0.50	0.50	2.90	2.90	2.90	2.89	2.90	3.03
0.75	0.25	3.46	3.47	3.46	3.46	3.46	3.51
1.00	0.00	4.03	4.03	4.03	4.03	4.03	4.03

Table 5 represents Calculated Energy Gap values value of Al_xGa_{1-x}N by Method-1, Method-2, Method-3, Method-4 and Additivity Principle

Table 6 Energy gap of In_xGa_{1-x}N

In Composition X	1-x	Energy gap Method-1 Ev	Energy gap Method-2 ev	Energy gap Method-3 ev	Energy gap Method-4 ev	Energy gap Additivity ev	Energy gap Reported E_g^{12} ev
0.00	1.00	1.11	1.11	1.11	1.11	1.11	1.11
0.25	0.75	0.91	1.10	0.91	0.91	0.908	0.95
0.50	0.50	0.70	1.10	0.70	0.71	0.705	0.73
0.75	0.25	0.50	0.40	0.50	0.50	0.503	0.55
1.00	0.00	0.30	0.30	0.30	0.30	0.30	0.30

Table 6 represents Calculated Energy Gap values value of In_xGa_{1-x}N by Method-1, Method-2, Method-3, Method-4 and Additivity Principle.

Table 7 Refractive index of $Al_xGa_{1-x}N$

Al Composition X	1-x	Refractive Index Method-1	Refractive Index Method-2	Refractive Index Method-3	Refractive Index Method-4	Refractive Index Additivity	Refractive Index n^{12} Reported
0.00	1.00	5.653	5.653	5.653	5.653	5.653	5.653
0.05	0.95	5.654	5.655	5.653	5.652	5.653	5.655
0.10	0.90	5.654	5.655	5.653	5.652	5.653	5.657
0.15	0.85	5.655	5.656	5.653	5.652	5.654	5.659
0.20	0.80	5.655	5.657	5.653	5.652	5.654	5.660
1.00	0.00	5.660	5.660	5.660	5.660	5.660	5.660

Table 7 represents Calculated Refractive index values value of $Al_xGa_{1-x}N$ by Method-1, Method-2, Method-3, Method-4 and Additivity Principle

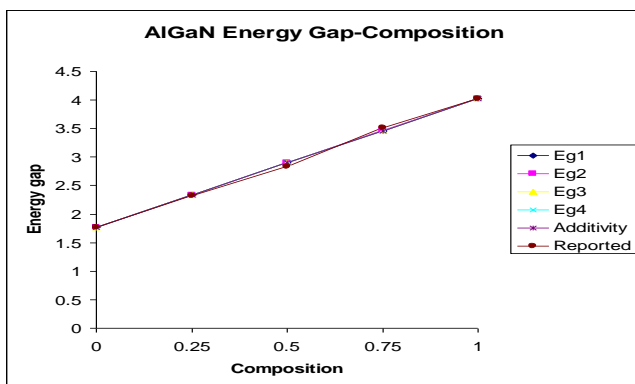


Fig 1 Explains Energy gap Methods at various Al Concentrations

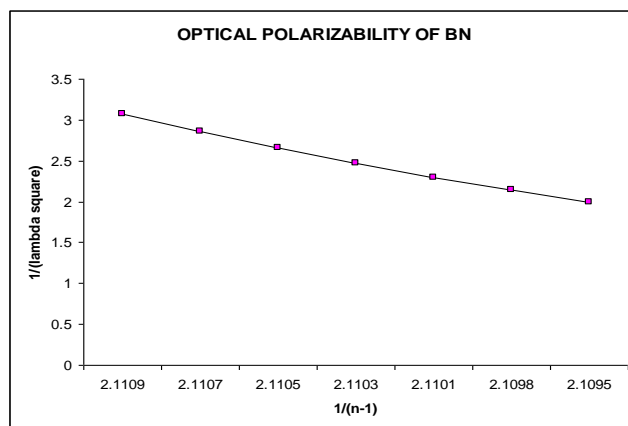


Fig 3 Explains Determination of Optical Polarizability in BN Compound

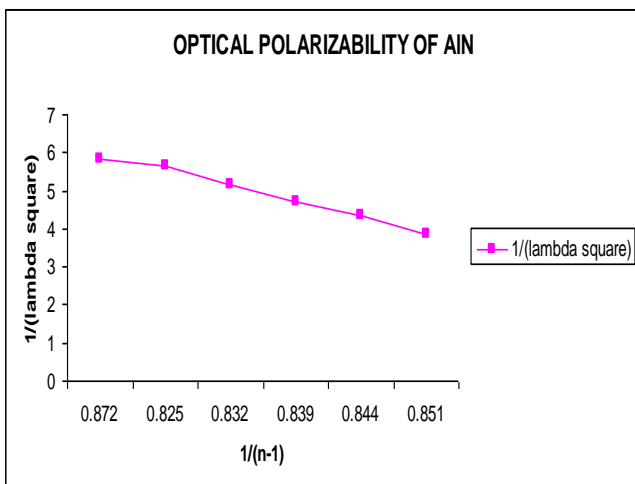


Fig 2 Explains Determination of Optical Polarizability in AlN Compound

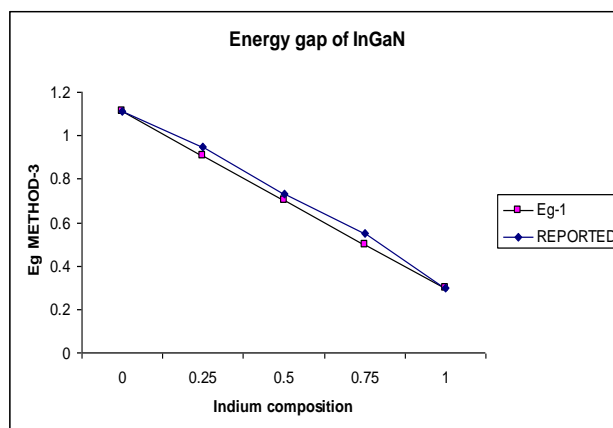


Fig 4 Explains Energy gap Method-1 with reported values in $In_xGa_{1-x}N$ Alloy. By increasing Indium Composition Energy gap has been decreased

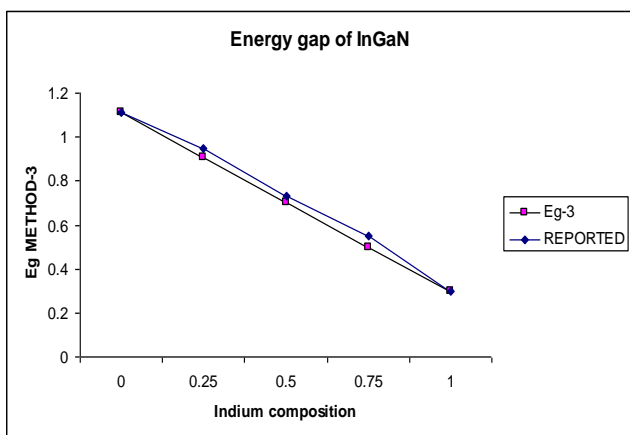


Fig 5 Explains Energy gap Method-3 with reported values in $\text{In}_x\text{Ga}_{1-x}\text{N}$ Alloy. By increasing Indium Composition Energy gap has been decreased

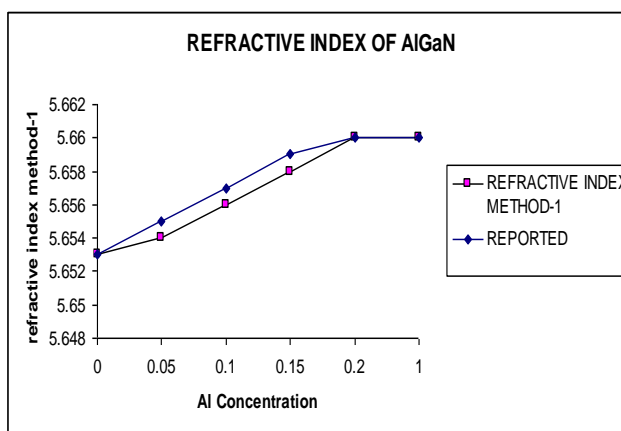


Fig 8 Explains REFRACTIVE INDEX Method-1 with reported values in $\text{Al}_x\text{Ga}_{1-x}\text{N}$ Alloy. By increasing Indium Composition REFRACTIVE INDEX has been increased

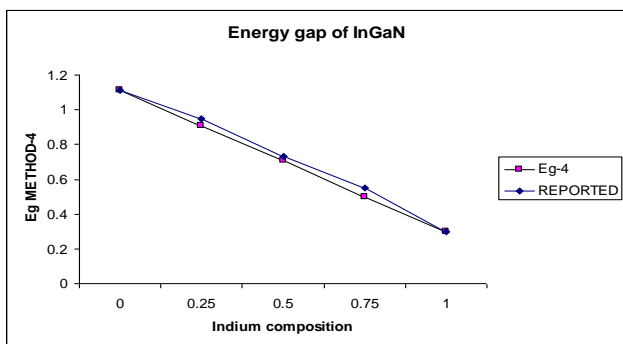


Fig 6 Explains Energy gap Method-4 with reported values in $\text{In}_x\text{Ga}_{1-x}\text{N}$ Alloy. By increasing Indium Composition Energy gap has been decreased

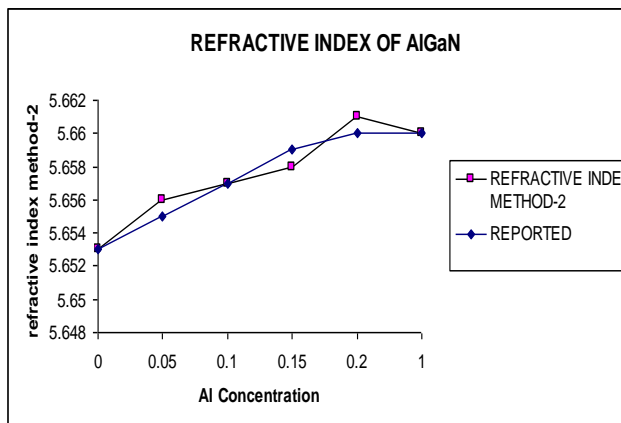


Fig 9 Explains REFRACTIVE INDEX Method-2 with reported values in $\text{Al}_x\text{Ga}_{1-x}\text{N}$ Alloy. By increasing Indium Composition REFRACTIVE INDEX has been increased

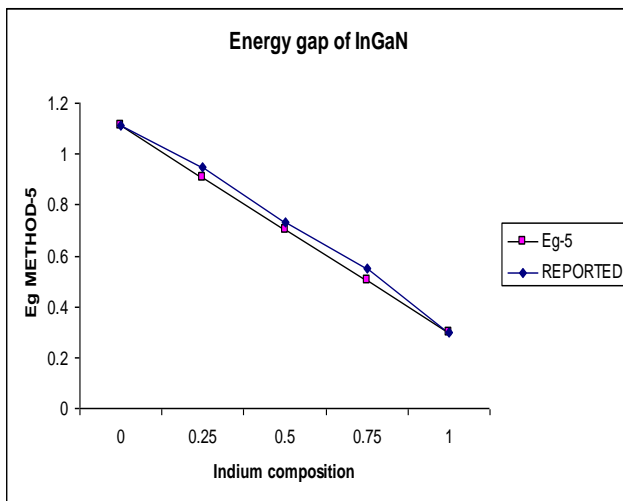


Fig 7 Explains Energy gap Method-5 with reported values in $\text{In}_x\text{Ga}_{1-x}\text{N}$ Alloy. By increasing Indium Composition Energy gap has been decreased

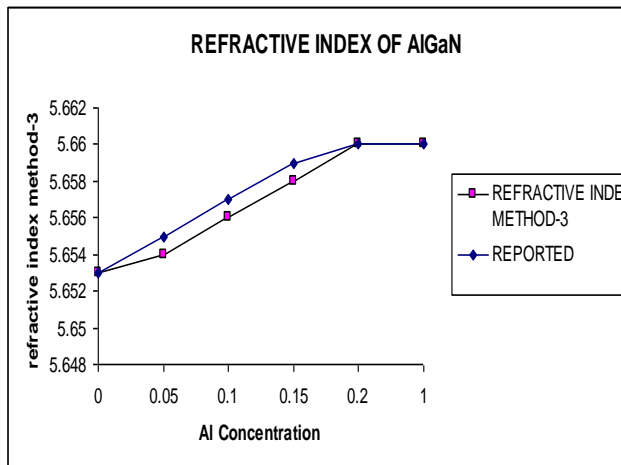


Fig 10 Explains REFRACTIVE INDEX Method-3 with reported values in $\text{Al}_x\text{Ga}_{1-x}\text{N}$ Alloy. By increasing Indium Composition REFRACTIVE INDEX has been increased

The applications of III-V Nitride Ternary Semiconductor Alloys of $\text{Al}_x\text{Ga}_{1-x}\text{N}$ Ternary Semiconductor Alloy, $\text{In}_x\text{Ga}_{1-x}\text{N}$ Ternary Semiconductor Alloy, $\text{Al}_x\text{In}_{1-x}\text{N}$ Ternary Semiconductor Alloy, $\text{GaAs}_x\text{N}_{1-x}$ Ternary Semiconductor Alloy, $\text{InAs}_x\text{N}_{1-x}$ Ternary Semiconductor Alloy and $\text{GaP}_x\text{N}_{1-x}$ Ternary Semiconductor Alloy as Electronic, Optical and Optoelectronic devices are determined by elementary material properties of Refractive index, Optical Polarizability, Absorption coefficient, Energy gap and Mobility. Photonic crystals, wave guides and solar cells require knowledge of refractive index and Energy gap of all above Arsenide Group alloys¹⁴.

The Energy gap of Semiconductor alloys determines Threshold for absorption of photons in semiconductors. Refractive index is measure of transparency of Semiconductor alloys to incident radiation. Refractive index and Energy gap of Ternary Semiconductor alloys has significant impact on Band structure. High absorption coefficient Semiconductor alloys can be used for fabricating in thin film hetero junction photovoltaic (PV) devices.

Narrow band gap semiconductor alloys of III-V Nitride Ternary Semiconductor Alloys of $\text{Al}_x\text{Ga}_{1-x}\text{N}$ Ternary Semiconductor Alloy, $\text{In}_x\text{Ga}_{1-x}\text{N}$ Ternary Semiconductor Alloy, $\text{Al}_x\text{In}_{1-x}\text{N}$ Ternary Semiconductor Alloy, $\text{GaAs}_x\text{N}_{1-x}$ Ternary Semiconductor Alloy, $\text{InAs}_x\text{N}_{1-x}$ Ternary Semiconductor Alloy and $\text{GaP}_x\text{N}_{1-x}$ Ternary Semiconductor Alloy are investigated for devices that allow one to attain frequencies that span over a wide range and attain Terahertz. Applications on these Ternary Semiconductor Alloy span from communications to biomedical engineering. Narrow band gap semiconductor alloys allow Hetero junction Bipolar Transistors to present terahertz (THz) operation capability.

Sensors of this type exploit the unique piezoelectric, polarization characteristics, as well as the high temperature stability of wide-band gap semiconductors in order to allow stable operation with high sensitivity. Using this material system one can also explore the possibility of developing fundamental sources operating in the Terahertz regime and employing Micro-Electro Mechanical Systems (MEMS) approaches.

Recent progress and new concepts using III-V Nitride Ternary Semiconductor Alloys of $\text{Al}_x\text{Ga}_{1-x}\text{N}$ Ternary Semiconductor Alloy, $\text{In}_x\text{Ga}_{1-x}\text{N}$ Ternary Semiconductor Alloy, $\text{Al}_x\text{In}_{1-x}\text{N}$ Ternary Semiconductor Alloy, $\text{GaAs}_x\text{N}_{1-x}$ Ternary Semiconductor Alloy, $\text{InAs}_x\text{N}_{1-x}$ Ternary Semiconductor Alloy and $\text{GaP}_x\text{N}_{1-x}$ Ternary Semiconductor Alloy and device concepts such quantum wells with very high mobility and plasma waves will lead in Terahertz detectors and emitters. Semiconductors of this type may also be used for other novel applications such as spintronics and field emission. Terahertz signal sources based on super lattices have explored applications cover a wide range of devices, circuits and components for communications, sensors and biomedical engineering.

Research on Physical properties of III-Nitride Semiconductor alloys is due to operating characteristics of Semiconductor devices depend critically on the physical properties of the constituent materials. The high electron mobility of InN, is due to its narrow band gap, makes this compound useful for very high-speed and low-power electronic and infrared optoelectronic devices.

The energy band gap of Group III-V Nitride Narrow Band gap Semiconductor alloys III-V Nitride Ternary Semiconductor Alloys of $\text{Al}_x\text{Ga}_{1-x}\text{N}$ Ternary Semiconductor Alloy, $\text{In}_x\text{Ga}_{1-x}\text{N}$ Ternary Semiconductor Alloy, $\text{Al}_x\text{In}_{1-x}\text{N}$ Ternary Semiconductor Alloy, $\text{GaAs}_x\text{N}_{1-x}$ Ternary Semiconductor Alloy, $\text{InAs}_x\text{N}_{1-x}$ Ternary Semiconductor Alloy and $\text{GaP}_x\text{N}_{1-x}$ Ternary Semiconductor Alloy reduces significantly from 1.11 to 0.30 by adding a small amount of Indium to $\text{In}_x\text{Ga}_{1-x}\text{N}$. These ternary alloys are used for manufacturing infrared detectors, gas sensors. The energy band gaps of above two alloys decrease rapidly leading to a strong disorder This occurs due to the large disparity in the electro negativity and the atomic size between In and Ga in $\text{In}_x\text{Ga}_{1-x}\text{N}$. The Indium atom and Gallium atom induces several perturbations in the host crystal.

The energy band gap of Group III-V Nitride wide Band gap Semiconductor alloys $\text{Al}_x\text{Ga}_{1-x}\text{N}$ increases significantly by adding small amount of Al to $\text{Al}_x\text{Ga}_{1-x}\text{N}$. The band gaps of these alloys are expected to vary from 1.77 eV (GaAs) to 4.03 eV.

The energy band gaps of above alloys increases rapidly leading to a strong disorder when a small amount of Ga atoms is replaced by Al. This occurs due to the large disparity in the electro negativity and the atomic size between Al and Ga in $\text{Al}_x\text{Ga}_{1-x}\text{N}$. The Al atom and Ga atom induces several perturbations in the host crystal of above alloys.

The binding which was totally covalent for the elemental Semiconductors, has an ionic component in III-V Nitride Ternary semiconductor alloys. The percentage of the ionic binding energy varies for various Semiconductor alloys. The percentage of ionic binding energy is closely related to electro negativity of the elements and varies for various compounds. The electro negativity describes affinity of electrons of the element. In a binding situation the more electro negative atoms will be more strongly bind the electrons than its partner and therefore carry net negative charge. The difference in electro negativity of the atoms in a compound semiconductor gives first measure for Energy gap. A more electro negative element replacing a certain lattice atom will attract the electrons from the partner more strongly, become more negatively charged and thus increase the ionic part of the binding. This has nothing to do with its ability to donate electrons to conduction band or accept electrons from the valence band.

Mobility at high doping concentration is always decreased by scattering at the ionized dopants. Band gap increases

with Electro negativity difference between the elements. Bond strength decreases with decrease of orbital overlapping. Large band gap in III-V Nitride Ternary Semiconductor Alloys of $\text{Al}_x\text{Ga}_{1-x}\text{N}$ Ternary Semiconductor Alloy, $\text{In}_x\text{Ga}_{1-x}\text{N}$ Ternary Semiconductor Alloy, $\text{Al}_x\text{In}_{1-x}\text{N}$ Ternary Semiconductor Alloy, $\text{GaAs}_x\text{N}_{1-x}$ Ternary Semiconductor Alloy, $\text{InAs}_x\text{N}_{1-x}$ Ternary Semiconductor Alloy and $\text{GaP}_x\text{N}_{1-x}$ Ternary Semiconductor Alloy is due to high degree of orbital overlapping. Electro negativity affects the width of the band gap. Electrons are more stabilized by more electro negativity atom. Pure semiconductors are located in Group 3 and group 4 of the periodic table. The band gaps of these materials are less influenced by electro negativity. They are influenced by configuration of crystal lattice, valence shell electrons and hybridization of orbitals.

Semiconductor Materials with higher absorption coefficients more readily absorb photons, which excite electrons into the conduction band. The absorption coefficient determines how far into a material light of a particular wavelength can penetrate before it is absorbed. In a material with a low absorption coefficient, light is only poorly absorbed, and if the material is thin enough, it will appear transparent to that wavelength. The absorption coefficient depends on the material and also on the wavelength of light which is being absorbed. III-V Nitride Ternary Semiconductor Alloys have a sharp edge in their absorption coefficient, since light which has energy below the band gap does not have sufficient energy to excite an electron into the conduction band from the valence band. Consequently this light is not absorbed.

On the other hand, if a plot of $h\nu$ versus $\alpha h\nu^{1/2}$ forms a straight line, it can normally be inferred that there is an indirect band gap, measurable by extrapolating the straight line to $\alpha=0$ axis. Measuring the absorption coefficient for Ternary Semiconductor Alloys gives information about the band gaps of the material. Knowledge of these band gaps is extremely important for understanding the electrical properties of a semiconductor. Measuring low values of Absorption coefficient (α) with high accuracy is photo thermal deflection spectroscopy which measures the heating of the environment which occurs when a Semiconductor sample absorbs light.

The energy levels adjust with alloy concentration, resulting in varying amount of absorption at different wavelengths in III-Nitride Ternary Semiconductor alloys This variation in optical properties is described by the material optical constants, commonly known as Refractive index (n). The optical constants shape corresponds to the material's electronic transitions. Thus, the optical constants become a "fingerprint" for the semiconductor alloys.

The band structure of III-V Nitride semiconductor alloys is similar since the tetrahedral bonds have the same structure as in Silicon or Germanium. In fact, the missing electron of the group III is provided by the column V element and

these bonds have a low ionicity. Most of III-V Nitride Ternary semiconductor alloys have direct band gap. The minimum photon energy that is needed to excite an electron into the conduction band is associated with the band gap of a material. When electron-hole pairs undergo recombination, photons are generated with energies that correspond to the magnitude of the band gap. A phonon is required in the process of absorption or emission in the case of an indirect band gap. There must be a direct band gap in applications of optical devices. The evaluation of refractive indices of semiconductor is of considerable importance for different applications, where the refractive index of the material is the key parameter for the device design.

The Refractive index of Group III-V $\text{Al}_x\text{Ga}_{1-x}\text{N}$ Ternary Semiconductor alloys modify significantly by adding a small amount of Al to GaN. These ternary alloys are used for manufacturing infrared detectors, gas sensors. This occurs due to the large disparity in the electro negativity and the atomic size between Al and Ga in $\text{Al}_x\text{Ga}_{1-x}\text{N}$.

These ternary alloys are used for manufacturing infrared detectors, gas sensors. This occurs due to the large disparity in the electro negativity and the atomic size

In III- $\text{Al}_x\text{Ga}_{1-x}\text{N}$ Ternary Semiconductor alloys replacing existing atom with high Atomic number results in Decreasing of Energy gap due to increase of charge carriers with increase of mobility and by replacing existing atoms of low atomic number result in Increase of Energy gap due to decrease of charge carriers transmitting from valence band to conduction band with decrease of mobility¹⁵.

References

- [1] <http://www.semiconductors.co.uk/nitrides.htm>
- [2] Deutsch T. Sunlight, Water and III-V Nitrides for Fueling the Future, PhD Thesis, Boulder, Colorado, 2006.
- [3] Irina Buyanova and Weimin Chen, eds. Physics and Applications of Dilute Nitrides (Taylor & Francis, New York, 2004).
- [4] Ayse Erol ed. Physics of Dilute III-V Nitride Semiconductors of $\text{Al}_x\text{Ga}_{1-x}\text{N}$ and Material Systems: Physics and Technology (Springer-Verlag Berlin-Heidelberg 2008).
- [5] Moss D, Akimov A V, Novikov S V, Campion R P, Staddon C R, Zainal N, Foxon C T, Kent A J, Elasto-optical properties of zinc-blende in $\text{In}_x\text{Ga}_{1-x}\text{N}$, J. Phys. D: Appl. Phys. 42 115412 (2009)
- [6] Novikov S.V , Staddon C.R, Akimov A.V, Campion R.P, Zainal N, Kent A.J, Foxon C.T, Chen C.H, K.M. Yu and W. Walukiewicz, Molecular beam epitaxy of crystalline and amorphous $\text{Al}_x\text{In}_{1-x}\text{N}$ layers with high As content, J. Cryst. Growth 311 3417 (2009)
- [7] Sergey V. Novikov, Chris R. Staddon, Andrey V. Akimov, Richard P. Campion, Norzaini Zainal, Anthony J. Kent, C. Thomas Foxon, Chien H. Chen, Kim M. Yu, Wladek

- Walukiewicz, Growth by Molecular Beam Epitaxy of GaAs_xN_{1-x} alloys with high As content for potential photoanode applications in hydrogen production, Mater. Res. Soc. Symp. Proc. 1167 1167-O04-07 (2009)
- [8] Novikov S.V , Zainal N, Akimov A.V, Staddon C.R, Kent A.J, Foxon C.T, MBE as a method for the growth of freestanding InAs_xN_{1-x} GaN layers and substrates, J. Vac. Sci. Technol. B 28 3 (2010)
- [9] Zainal, P. Walker, A.J Kent, Modelling of GaP_xN_{1-x} Resonant Tunnel Diode Structures, Phys. Status Solidi (C), DOI 10.1002/pssc.200983543, (2010)
- [10] Murthy, V.R, and Sathya Latha K.C Extension of principle of additivity and refractive indices of ternary compounds- National seminar on Solid state spectroscopy, SV University, Tirupathi, August, 2001- Communicated to ASEAN journal on Science and Technology for development.
- [11] CRC Press Online: CRC Handbook of Chemistry and Physics, 92st Edition of The CRC Handbook of Chemistry and Physics is in its 92nd edition (published June 15, 2011 by CRC Press).
- [12] G. M. Laws¹, E. C. Larkins¹, I. Harrison¹, C. Molloy², and D. Somerford²
- [13] Improved Refractive index formulas for the In_xGa_{1-x}N and Al_xGa_{1-x}N J. Appl. Phys. **89**, 1108 (2001); <http://dx.doi.org/10.1063/1.1320007>
- [14] Zeng, S. W.; *et al* "Substantial photo-response of InGaN p-i-n homojunction solar cells". *Semi cond. Sci. Technol* **24**: 055009. doi:10.1088/0268-1242/24/5/055009. (2009).
- [15] Sun, X.; *et al*. "Photoelectric characteristics of metal/InGaN/GaN heterojunction structure". *J. Phys. D* **41**: 165108. doi:10.1088/0022-3727/41/16/165108. (2008).
- [16] Dirk V. P. McLaughlin and J.M. Pearce (2012). "Analytical Model for the Optical Functions of Indium Gallium Nitride with Application to Thin Film Solar Photovoltaic Cells"(2008).
-